

Raman spectroscopic study of PbCO_3 at high pressures and temperatures

Robert Minch · Leonid Dubrovinsky ·
Alexandr Kurnosov · Lars Ehm · Karsten Knorr ·
Wulf Depmeier

Received: 22 December 2008 / Accepted: 30 April 2009
© Springer-Verlag 2009

Abstract Cerussite (PbCO_3) has been investigated by high-pressure and high-temperature Raman spectroscopy up to pressures of 17.2 GPa and temperatures of 723 K. Two pressure induced phase transitions were observed at about 8.0(2) and 16.0(2) GPa, respectively. The post-aragonite transition (PbCO_3 -II) at 8.0(2) GPa is accompanied by softening of the ν_2 -out-of-plane mode of the CO_3^{2-} group and disappearance of the B_{1g} (ν_4 -in-plane band of the CO_3^{2-} group) mode. Stronger shifts of the carbonate group modes after the phase transition suggest that the new structure is more compressible. The formation of a second high-pressure polymorph begins at about 10 GPa. It is accompanied by the occurrence of three new bands at different pressures and splitting of the ν_1 -symmetric C–O stretching mode of the CO_3^{2-} group. The transitions are reversible on pressure release. A semi-quantitative phase

diagram for PbCO_3 as a function of pressure and temperature is proposed.

Keywords Cerussite · Raman spectroscopy · High pressure · High temperature · Phase transition

Introduction

Carbonates belong to the most abundant Earth materials after silicates and play an important role in the Earth's carbon cycle (Janzen 2004). The total amount of carbon in the atmosphere, oceans and other near-surface reservoirs is negligible compared to the amount stored in the Earth's mantle (Javoy et al. 1982). Therefore, understanding where and how carbon is stored within the Earth's interior is of great interest. Silicates have been proposed as a possible host for carbon in the Earth's interior (Green 1972). However, it has recently been shown that the solubility of carbon in silicates at mantle conditions is low. It has been proposed, instead, that most of the Earth's carbon is likely to be stored in the form of high-pressure Mg and/or Ca carbonates (Kepler et al. 2003). Isshiki et al. (2004) found that magnesite (MgCO_3) does not dissociate at high pressure and temperature, but transforms to an unknown structure at about 115 GPa and 2,100–2,200 K. CaCO_3 has been found to be stable up to 192 GPa showing a sequence of pressure induced phase transitions (Ono et al. 2005a, 2007). Recently, investigations of mineral inclusions in diamonds from the lower part of the transition zone revealed carbonate minerals, thereby demonstrating that transport to great depths and storage of carbonates is possible (Brenker et al. 2007).

Besides their geological relevance, carbonates attracted considerable interest as possible storage phases for the

R. Minch (✉) · W. Depmeier
Institut fuer Geowissenschaften, CAU zu Kiel,
Olshausenstr. 40, 24098 Kiel, Germany
e-mail: robert@min.uni-kiel.de

L. Dubrovinsky · A. Kurnosov
Bayerisches Geoinstitut, Universitaet Bayreuth,
95220 Bayreuth, Germany

L. Ehm
Mineral Physics Institute, Stony Brook University, 255 Earth and
Space Science Building, Stony Brook, NY 11794-2100, USA

L. Ehm
Brookhaven National Laboratory, National Synchrotron Light
Source, 75 Brookhaven Avenue, Upton, NY 11973-5000, USA

K. Knorr
Bruker AXS-GmbH, XRD Marketing,
Oestliche Rheinbrueckenstr. 49, 76187 Karlsruhe, Germany

sequestration of anthropogenic CO₂ in geologic formations (IPCC 2005; Gibbins and Chalmers 2008; Bachu 2008).

At ambient conditions all carbonates of bivalent cations exist in two polymorphic forms with the calcite (CaCO₃, MgCO₃, CdCO₃, ZnCO₃, FeCO₃) or aragonite (CaCO₃, BaCO₃, SrCO₃, PbCO₃) structure type. Insight into the high-pressure behavior of aragonitic CaCO₃ can be gained by investigating isostructural minerals with larger cations, such as BaCO₃, PbCO₃, and SrCO₃. Whereas these minerals cannot claim any general geological interest as major constituents of the Earth's crust or mantle, the *P*–*T* conditions of the phase transitions in these compounds are generally lower than in CaCO₃ and experimentally easier accessible (pressure-homologous rule). Pb as a p-group element has a lone electron pair in its divalent state which sets it apart from the closed-shell earth-alkaline cations. The lone pair occupies an inert orbital in the ligand sphere and can be stereochemically active (Siidra et al. 2008). Therefore, it is interesting to see whether this special electronic configuration results in any kind of untypical high-pressure behavior. Various aspects of the behavior of CaCO₃, SrCO₃, PbCO₃ and BaCO₃ under extreme conditions have already been investigated.

Lin and Liu (1997b) found that both, cerussite (PbCO₃) and strontianite (SrCO₃), undergo a phase transition to a post-aragonite phase, at 17 and 35 GPa, respectively. A Raman spectrum of a PbCO₃ sample quenched from 22 GPa/1,000 K looked identical to that observed at 22 GPa and room temperature and also at above 4 GPa and about 1,273 K. This strongly suggests negative slope of the phase boundary in a *P*–*T* diagram. From single crystal X-ray diffraction at 7.2 GPa it was found (Holl et al. 2000) that BaCO₃ undergoes a first-order transition to a trigonal structure. A high-pressure IR-spectroscopic study of PbCO₃ up to 41 GPa (Catalli et al. 2005) showed a phase transition from an orthorhombic to a trigonal structure. The spectral changes observed are consistent with the formation of a small, trigonal unit cell, with space group $\bar{P}31c$ and two formula units per unit cell, corresponding to the high-pressure phase of BaCO₃-III (Holl et al. 2000). Using a combination of ab initio techniques and high-pressure experiments, Oganov et al. (2006) proposed the structure of the post-aragonite phase of CaCO₃. Its structure is similar to those of the high-pressure phases of SrCO₃ (Ono et al. 2005b) and of BaCO₃-IV (Ono 2007). It is difficult to compare the results of the different authors because the experiments were carried out under quite different conditions. Following the pressure-homologous rule, according to which isostructural compounds containing different cations undergo similar phase transitions, but at higher pressures, when the cation radii decrease (Brown 1975), it was suggested that all carbonates with aragonite structure should have similar phase diagrams, but with different *P*–*T*

conditions. It is of interest to check out whether the pressure homologous rule is also applicable to the particular case of PbCO₃ with its lone pair effect and whether the construction of a general phase diagram for carbonates with divalent cations is possible.

Here we report the results of our pressure and temperature-dependent Raman-spectroscopic experiments on PbCO₃ which are then used to construct a tentative *P*–*T* phase diagram of cerussite.

Experimental

Extra pure PbCO₃ was used for the experiments (99.999%, Alfa Aesar GmbH). The Raman spectra in the 100–1,200 cm⁻¹ frequency range were collected using a LABRAM system spectrometer with a 514.5 nm Ar⁺ ion laser as the excitation light source. The scattered light was collected in backscattering geometry using a liquid nitrogen cooled CCD detector with a resolution of $\pm 2\text{cm}^{-1}$. The high-pressure Raman spectra were obtained using the BGI-type diamond anvil cell (DAC), a 25× microscope objective and three accumulations with 60 s integration time. The investigated range was extended to 1,600 cm⁻¹ for the characterization of the starting material.

We used 16-sided type Ia Raman ultra low-fluorescence diamonds with a culet diameter of 300 μm. The pressure was determined by the ruby fluorescence method following the Piermarini pressure scale (Piermarini et al. 1975). Neon was used as pressure transmitting medium. A Re gasket was pre-indented and a hole with 150 μm diameter drilled at the center as a sample chamber. Both, Raman spectra and the ruby fluorescence, were measured at the same spot.

The experiments were carried out under isobaric or isothermal conditions, respectively. An external resistively heated DAC was used for the high-temperature experiments. The temperature was controlled by Pt-thermocouples. The uncertainties of the pressure and temperature measurements are estimated to be 0.2 GPa and 3 K, respectively, both on compression and decompression. The positions of the Raman peaks were determined by fitting Lorentzian functions to the spectra using the OPUS 5.5 (Bruker, 2004) version software package.

Results

Under ambient conditions, lead carbonate (PbCO₃) crystallizes in the aragonite structure with space group *Pnma*. The factor group analysis predicts 30 Raman active ($9A_{1g} + 6B_{1g} + 6B_{2g} + 9B_{3g}$) and 18 IR active ($8B_{1u} + 5B_{2u} + 5B_{3u}$) vibrational modes. We observed 14 Raman modes in the range 100–1,600 cm⁻¹, in good

agreement with Lin and Liu (1997b). These modes can be divided into four main regions as shown in Table 1.

Isothermal (293 K) compression

Raman spectra of the out-of-plane (ν_2), in-plane (ν_4) and symmetric stretching (ν_1) bands of lead carbonate on compression are shown in Fig. 1. The onset of two new peaks ν_2' and ν_1' (see Fig. 1) is observed at pressures of about 8.9(2) and 10.2(2) GPa, respectively. The positions of the Raman bands corresponding to the internal modes as a function of pressure up to 15.4(2) GPa, are shown in Fig. 2. Three cell loadings and experimental runs were

done in order to check the reproducibility of the experiments and to verify the behavior of the ν_2 mode. In Fig. 2a–d results of the three experiments are presented in different colors to show the frequency variations of bands at different pressures and different runs. Results of all runs are in a good agreement and ν_2 shows, indeed, a mode softening. The first run was carried out up to 9 GPa, the second up to 14 GPa and the third up to 15.6 GPa. The results of the linear fit to the data from the third experiment will be discussed further below. The position of the ν_1 band increases linearly with increasing pressure (Fig. 2a) up to 15.4 GPa with a rate of 2.53(4) $\text{cm}^{-1}/\text{GPa}$. The ν_2 out-of-plane bending mode shows a mode softening (Fig. 2b).

Table 1 Assignment of Raman bands of PbCO_3 at ambient conditions based on the space group $Pnma$

Region (cm^{-1})	Wavenumber (cm^{-1})	Assignment (Frech and Wang 1980)
100–230 External modes	114.6, 130.2, 148.3, 173 and 218.5	Modes are associated with translations of the Pb^{2+} ions and CO_3^{2-} groups along different axis and with rotation of CO_3^{2-} groups
600–900 Internal modes	671.2	(1) B_{3g} (ν_4 -in-plane band of CO_3^{2-} groups)
	675.8	(2) A_{1g} (ν_4 -in-plane band of CO_3^{2-} groups)
	683.8	(3) B_{2g} (ν_4 -in-plane band of CO_3^{2-} groups)
	696.6	(4) B_{1g} (ν_4 -in-plane band of CO_3^{2-} groups)
	839.2	(5) A_{1g} (ν_2 -out-of-plane band of CO_3^{2-} groups)
900–1,100	1,054.5	(6) A_{1g} (ν_1 -symmetric C–O stretching of CO_3^{2-} groups)
1,200–1,600	1,371.3	A_{1g} (ν_3 -asymmetric C–O stretching of CO_3^{2-} groups)
	1,421.3	
	1,478.1	

Fig. 1 Raman spectra of PbCO_3 out-of-plane (ν_2) and in-plane (ν_4) bending of CO_3^{2-} groups as a function of pressure at room temperature: 1 B_{3g} (ν_4 -in-plane band), 2 A_{1g} (ν_4 -in-plane band), 3 B_{2g} (ν_4 -in-plane band), 4 B_{1g} (ν_4 -in-plane band). The insets highlight the ν_2' band between 8.9 and 15.4 GPa and the ν_1 symmetric stretching vibrations as function of pressure. An arrow denotes the signal of the diamond around 740 cm^{-1} , which disappears with pressure. Spectra are vertically offset for clarity

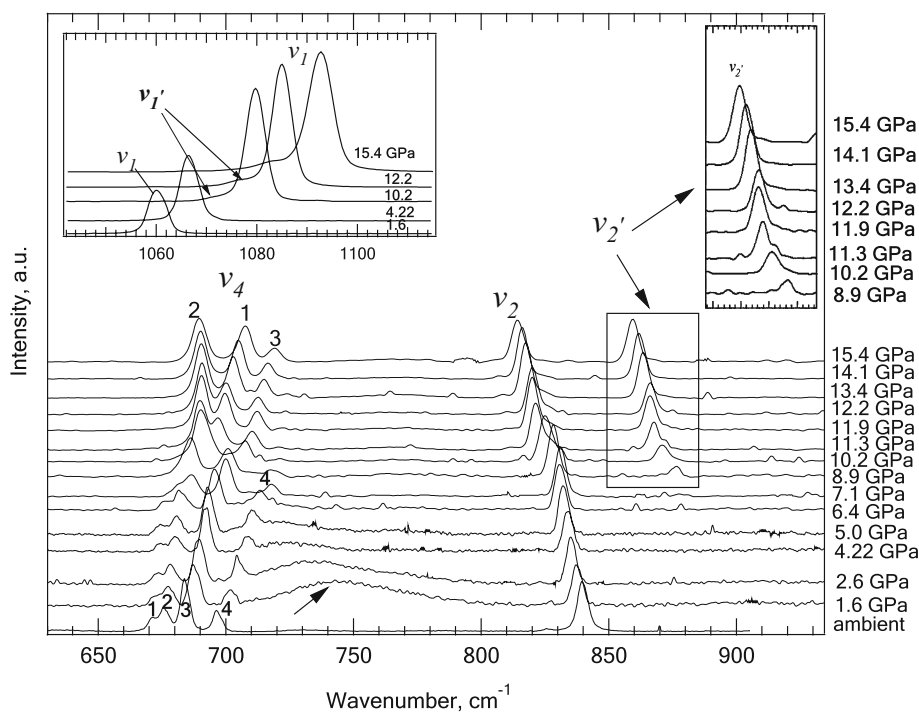
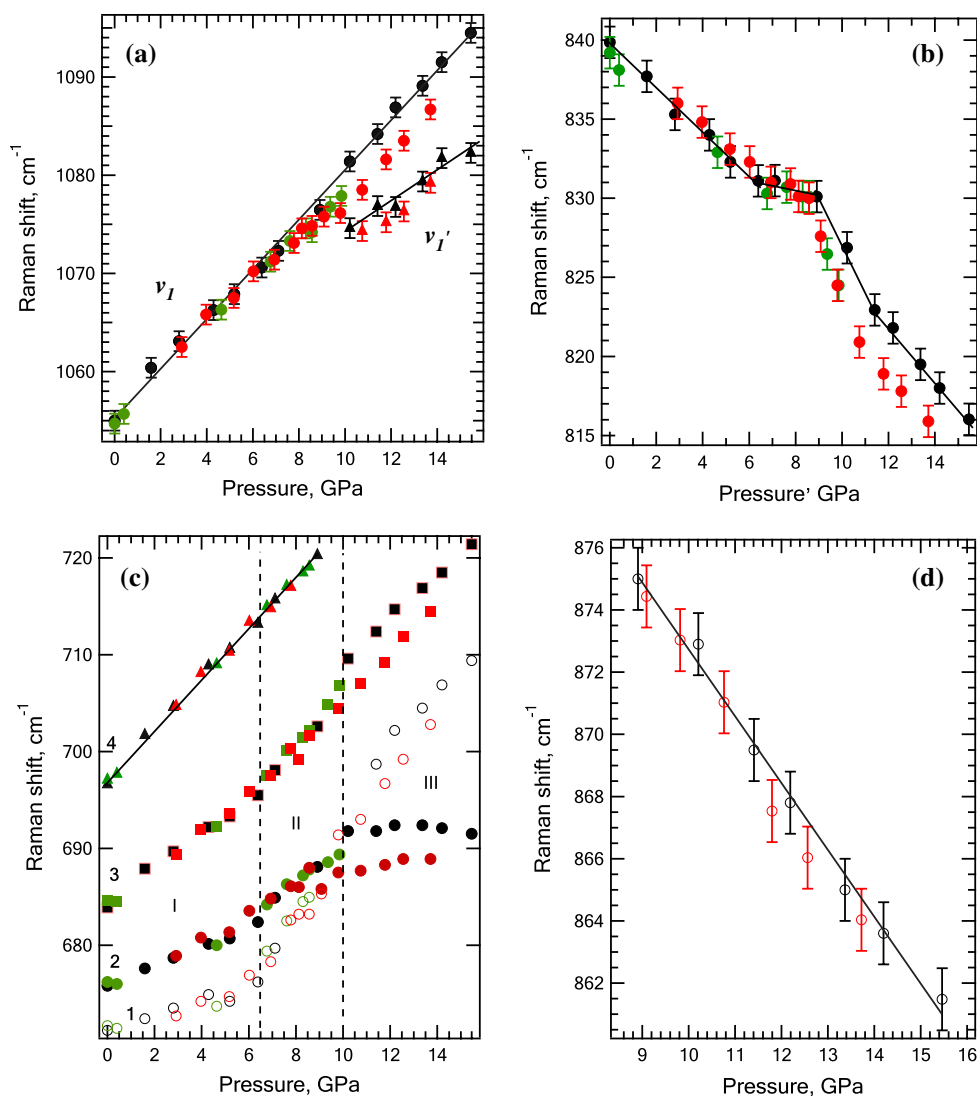


Fig. 2 Pressure-induced mode shifts of internal vibrations on compression at ambient temperature in different experiments runs: **a** ν_1 (filled circle), ν_1' (filled triangle) asymmetric vibrations; **b** ν_2 -out-of-plane band (filled circle); **c** ν_4 -in-plane band [$1 B_{3g}$ (open circle), $2 A_{1g}$ (filled circle), $3 B_{2g}$ (filled square), $4 B_{1g}$ (filled triangle)]; **d** ν_2' -out-of-plane band (open circle). *I, II, III* indicate the supposed fields of the existence of phases I, II, III. Colors indicate the run number of the experiments: green the first, red the second and black the third. The first run was carried out up to 9 GPa, the second up to 14 GPa and the third up to 15.6 GPa. The size of the symbols corresponds to errors in Raman shift and pressure in **c** and in **P** in **a, b, d**



A negative linear slope of $-1.38(7) \text{ cm}^{-1}/\text{GPa}$ is observed up to 6.4 GPa. Thereafter the peak position stays roughly constant up to 8.8 GPa, dv/dP being $-0.32(5) \text{ cm}^{-1}/\text{GPa}$. From about 8.8(2) GPa up to 11.5(2) GPa the negative average slope is much stronger, $-2.86(20) \text{ cm}^{-1}/\text{GPa}$. A last change of the slope is observed at 11.5(2) GPa where dv/dP decreases to $-1.74(4) \text{ cm}^{-1}/\text{GPa}$.

The behavior of the ν_4 -in-plane bending modes consisting of four lines (Table 1) is non-monotonic (Fig. 2c). Only B_{1g} increases linearly with increasing pressure and disappears at about 8.9(2) GPa (4 in Fig. 1, triangles in Fig. 2c). The behavior of the modes is listed quantitatively in Table 2. Three pressure ranges can be distinguished in which the ν_4 -in-plane bands have different dv/dP values. Only small hysteresis effects could be observed upon pressure release within the uncertainty of our experiment. The B_{1g} in-plane bending re-appears at some lower

Table 2 Comparison of the dv/dP values of ν_4 modes in different pressure ranges

ν_4 Mode	Pressure range (GPa)	dv/dP ($\text{cm}^{-1}/\text{GPa}$)
1 (B_{3g})	0–6.40	0.72 (9)
	6.4–12	4.40 (15)
	12–15.4	2.24 (11)
2 (A_{1g})	0–6.4	0.98 (3)
	6.4–10.4	2.33 (18)
	10.4–15.4	−0.02 (9)
3 (B_{2g})	0–6.4	1.74 (9)
	6.4–12	3.44 (20)
	12–15.4	2.15 (8)
4 (B_{1g})	0–9.0	2.60 (6)

Standard deviations of the linear fits to the dv/dP values are given in parentheses

pressure of about 8.49(20) GPa upon decompression (Fig. 3); ν_2' and ν_1' disappear at 8.5(2) GPa, instead of 10.2(2) GPa upon compression.

Isobaric (7.6(2) GPa) heating experiments

A second set of experiments was performed under isobaric conditions at 7.6(2) GPa, but variable temperatures up to 723 K. Figure 4 shows the evolution of the ν_4 (in-plane) and ν_2 (out-of-plane)-bands with changing temperature.

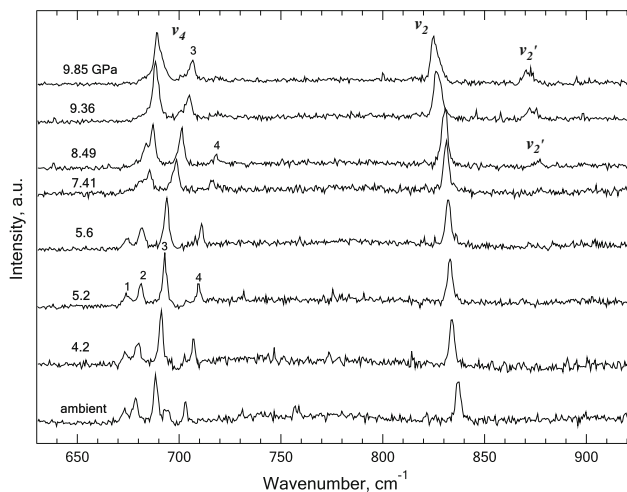


Fig. 3 Raman spectra of ν_2 -out-of-plane and ν_4 -in-plane internal vibrations upon decompression at ambient temperature: 1 B_{3g} (ν_4 -in-plane band), 2 A_{1g} (ν_4 -in-plane band), 3 B_{2g} (ν_4 -in-plane band), 4 B_{1g} (ν_4 -in-plane band). Spectra are vertically offset for clarity

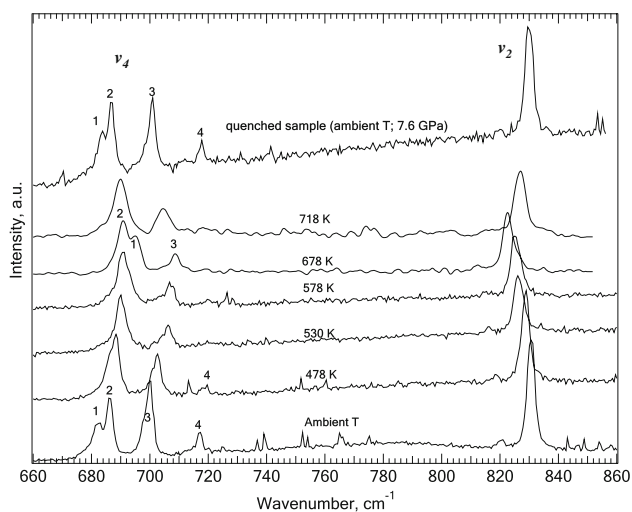


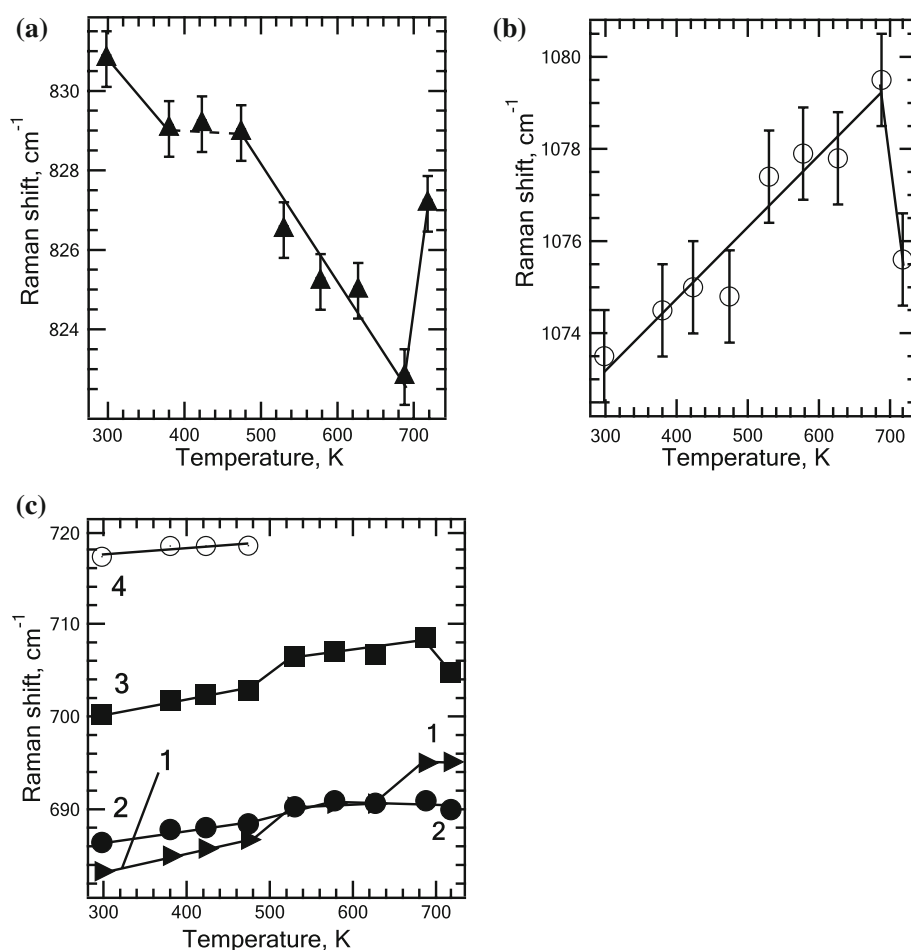
Fig. 4 Raman spectra of the internal modes (ν_2 -out-of-plane band and ν_4 -in-plane band) of $PbCO_3$ at 7.6(2) GPa as a function of temperature: 1 B_{3g} (ν_4 -in-plane band), 2 A_{1g} (ν_4 -in-plane band), 3 B_{2g} (ν_4 -in-plane band), 4 B_{1g} (ν_4 -in-plane band). Spectra are vertically offset for clarity

The disappearance of the ν_4 - B_{1g} band (4) is observed at about 500 K, which is remarkably similar to the behavior of this band in the isothermal high-pressure experiments (see Fig. 1 at about 9 GPa). All mode shifts are reversible. Bands return to their initial positions upon quenching to ambient temperature. The temperature dependence of the internal modes at 7.6(2) GPa is shown in Fig. 5. The change in frequencies of the ν_2 out of plane bending (Fig. 5a) is similar to the ambient temperature high-pressure experiments (Figs. 2b, 5a). Again, a temperature induced mode softening is observed. However, the peak position remains almost constant in the temperature range from 383(3) to 473(3) K, resembling the behavior under isothermal conditions in the pressure range from 6.4(2) to 8.8(2) GPa (Fig. 2b). This observation lends itself to the idea that the processes taking place are quite similar despite the rather different conditions. The slope changes above 473 K and dv/dP becomes more negative with increasing temperature. A dramatic change is observed at 673(3) K where the slope turns steeply positive. The behavior of the ν_1 -symmetric stretching mode of the CO_3^{2-} group till 673 K is similar to that upon isothermal compression (Figs. 5b, 2a). At 673(3) K a change of the slope of the ν_1 band is observed. The behavior of the ν_4 modes is more difficult to interpret (Fig. 5c). Bands 1, 2 and 3 increase monotonously with increasing temperature up to 473(3) K, followed by a slope change to higher dv/dP values up to 523(3) K, and then return to the low-temperature value. At 673(3) K a second change of the slope is observed. The disappearance of band 4 (B_{1g}) takes place at 473(3) K, and is similar to the behavior observed at about 9 GPa and ambient temperature (Fig. 2c). As there is only one data point available above 700 K, the observed dramatic change of the behavior of the ν_1 and ν_2 bands is difficult to interpret, and its mere existence should be considered with due caution.

Isobaric (15.6(2) and 17.2(2) GPa) heating experiments

A third series of experiments was performed under still isobaric conditions but at temperatures up to 500(3) K at 15.6(2) GPa and up to 544(3) K at 17.2(2) GPa. The Raman spectra of the internal modes as function of temperature and the mode shifts are shown in Figs. 6 and 7 for the experiments at 15.6(2) and in Figs. 8 and 9 for those at 17.2(2) GPa. Two additional bands appeared during heating (marked 7 and 8 in Fig. 6a). They could be assigned to internal modes, and may be associated with the appearance of phase III. The splitting of the ν_1' and ν_1 positions becomes more distinct (Fig. 6b). Only for the ν_1' mode, the observed change of the slope was significant in the temperature range from 323(3) to 330(3) K (Fig. 7c). All other modes change monotonously.

Fig. 5 Temperature dependence of the internal Raman mode frequencies at 7.6(2) GPa: **a** ν_2 -out-of-plane band (filled triangle), **b** ν_1 -asymmetric stretching vibration (open circle), **c** ν_4 -out-of-plane band [1 B_{3g} (filled right triangle), 2 A_{1g} (filled circle), 3 B_{2g} (filled square), 4 B_{1g} (open circle)]. The size of the symbol corresponds to the errors in Raman shift and T in **a**, **b** and in T in **a**, **b**



The behavior of almost all the bands is similar in the case of the experiment performed at 17.2(2) GPa and temperatures up to 544 K (Fig. 8). Increasing temperature virtually leaves the position of the bands unaffected, displacements being less than 1 cm^{-1} (Fig. 9), and the number of bands unchanged. Thus, we conclude that the phase III has already been formed. Its formation was accompanied by the occurrence of three new bands (ν_2' , 7, 8) at different pressures and splitting of the ν_1 -symmetric C–O stretching mode of the CO_3^{2-} group (Fig. 8). Direct qualitative comparison of the spectra obtained at room temperature and 17.2(2) GPa (Fig. 8) and 15.6(2) GPa and 323(3) K (Fig. 6), respectively, shows the same profile and number of bands. This implies that PbCO_3 has the same structure under both conditions. The frequencies of all modes change monotonously with increasing temperature (Fig. 9). A change of the slope of the temperature dependence of the ν_4 internal vibrations (Fig. 9a) was observed in the 330(3)–350(3) K temperature range.

Isothermal (544(3) K) decompression

Isothermal decompression was carried out in the last set of experiments. The pressure was released with 1 GPa steps at

a constant temperature of 544(3) K. The two additional bands (marked 7 and 8 in Fig. 10), which had appeared during compression at 17.2(2) GPa (Fig. 8b), disappear below 12.2(2) GPa, as shown in Fig. 10. The disappearance upon decompression and appearance upon compression (Figs. 1, 2d) of the ν_2' out-of-plane band takes place at about 10 GPa. The ν_1' band disappears just below 12.2(2) GPa upon isothermal decompression at 544(3) K (Fig. 10b). Figure 11 shows the Raman bands of PbCO_3 at 544(3) K as a function of pressure. The mode shifts of the bands 7, 8 and ν_4 - B_{1g} are not shown. Bands 7 and 8 are virtually pressure-independent. ν_4 - B_{1g} is very weak, in fact hardly distinguishable from the noise. It is therefore difficult to determine its precise position. The dv/dP values are given in Table 3. Mode softening of ν_2 and ν_2' was observed in the whole pressure range (Fig. 11b, d). The slope dv_2/dP changes at pressures of about 13.0(2) and 7.2(2) GPa. The second change of the slope suggests the return to the orthorhombic starting phase. The same behavior is observed for ν_4 bands marked 1, 2, 3 in Fig. 11a, namely the same stable value of dv/dP in the 15.0–13.0 GPa pressure range and change of the slope at about 13.0(2) and 7.2–7.8 GPa. The disappearance of the

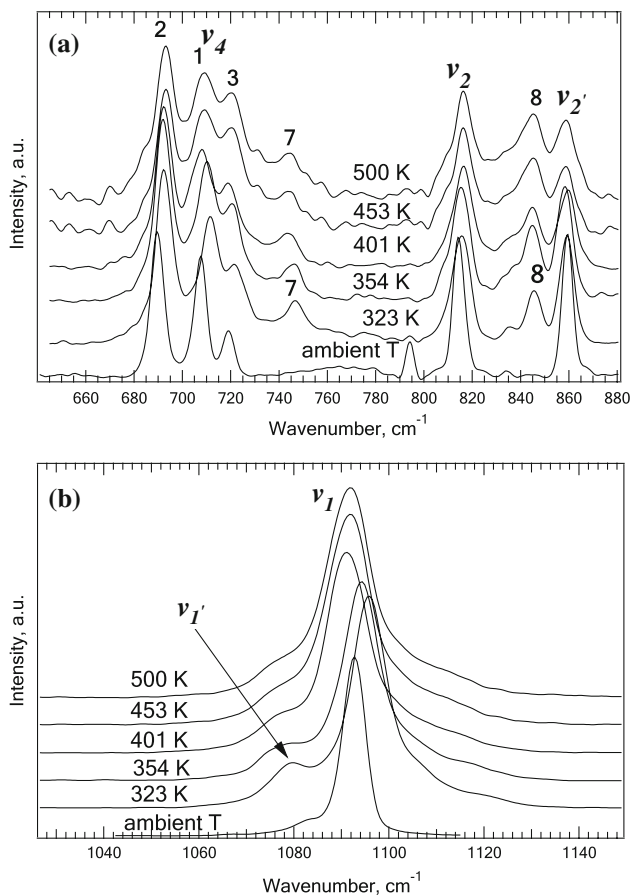
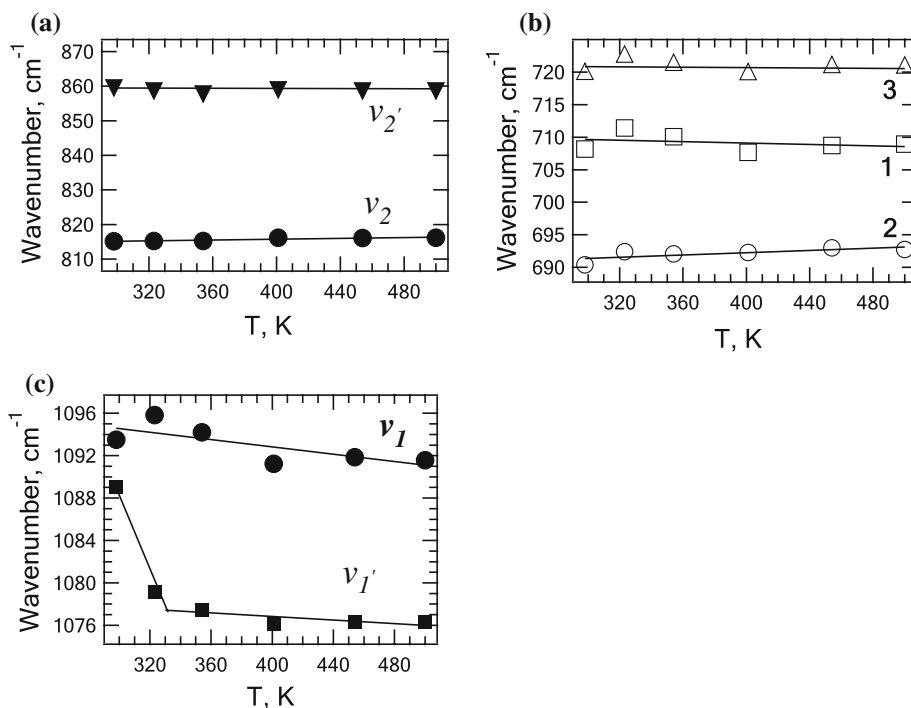


Fig. 6 Raman spectra of internal vibrations at 15.6(2) GPa as a function of temperature: **a** ν_4 -in-plane band ($1 B_{3g}$, $2 A_{1g}$, $3 B_{2g}$); ν_2 , ν_2' -out-of-plane bands; 7, 8 new bands; **b** ν_1 , ν_1' -asymmetric stretching. Spectra are vertically offset for clarity

Fig. 7 Temperature dependence of Raman frequencies of internal vibrations at 15.6(2) GPa: **a** ν_2' (filled inverted triangle), ν_2 (filled circle), **b** ν_4 -in-plane band [$1 B_{3g}$ (open square), $2 A_{1g}$ (open circle), $3 B_{2g}$ (open triangle)], **c** ν_1 (filled circle) and ν_1' (filled square). Errors in the wavenumber and T are estimated to be smaller than the graphical symbols used



bands 7 and 8 and of ν_1' , and changes in the slope at about 13.0(2) GPa suggest a III \rightarrow II phase transition at these conditions.

Discussion

There is no generally accepted classification for the high-pressure forms of carbonates crystallizing with the aragonite type structure. In particular, the term ‘post-aragonite’ is not well-defined. For all aragonite-type compounds more than one high-pressure polymorph is reported and which of them should be described as ‘post-aragonite’ is a matter of debate. We therefore consider it more appropriate to apply the nomenclature proposed by Ono for BaCO_3 (Ono 2007) for the following discussion.

At ambient temperature two high-pressure phase transitions of PbCO_3 (Phase I) have been identified: the first one at about 8 GPa (Phase I \leftrightarrow II) and the second at 17 GPa (II \leftrightarrow III). In the previous work of Lin and Liu (1997b) only the phase transition at 17 GPa and room temperature was observed. In our study four bands were determined in the wavenumber range from 650–700 cm^{-1} (Fig. 1: bands 1, 2, 3, 4), at variance with the spectra of Lin and Liu (1997b) (only one at 682 cm^{-1}). The B_{1g} band, which we observed at 696.6 cm^{-1} and the disappearance of which would indicate the I \rightarrow II phase transition, was not detected in the previous investigation. Lin and Liu (1997b) proposed the formation of their phase II (phase III in our work) by the appearance of the two ‘likely’ bands for

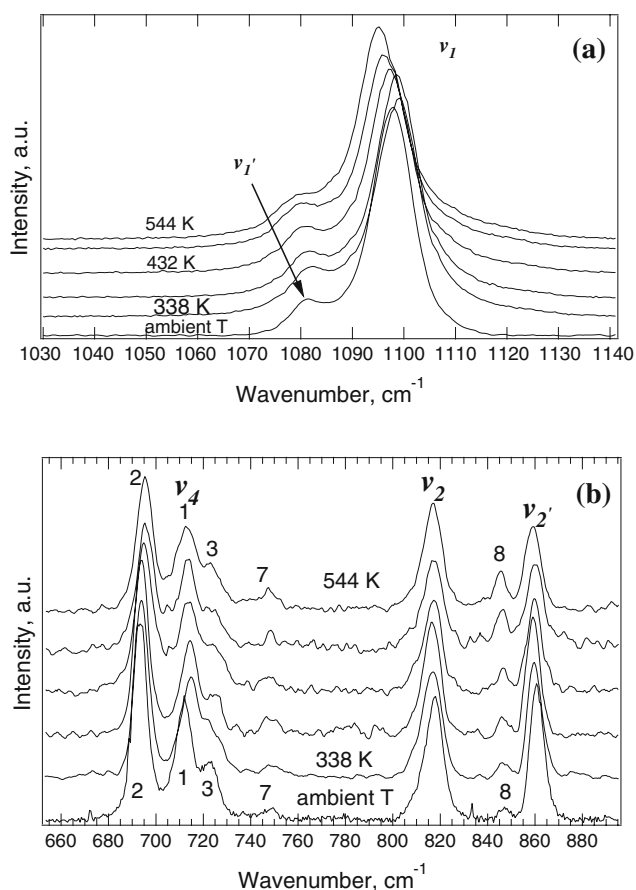
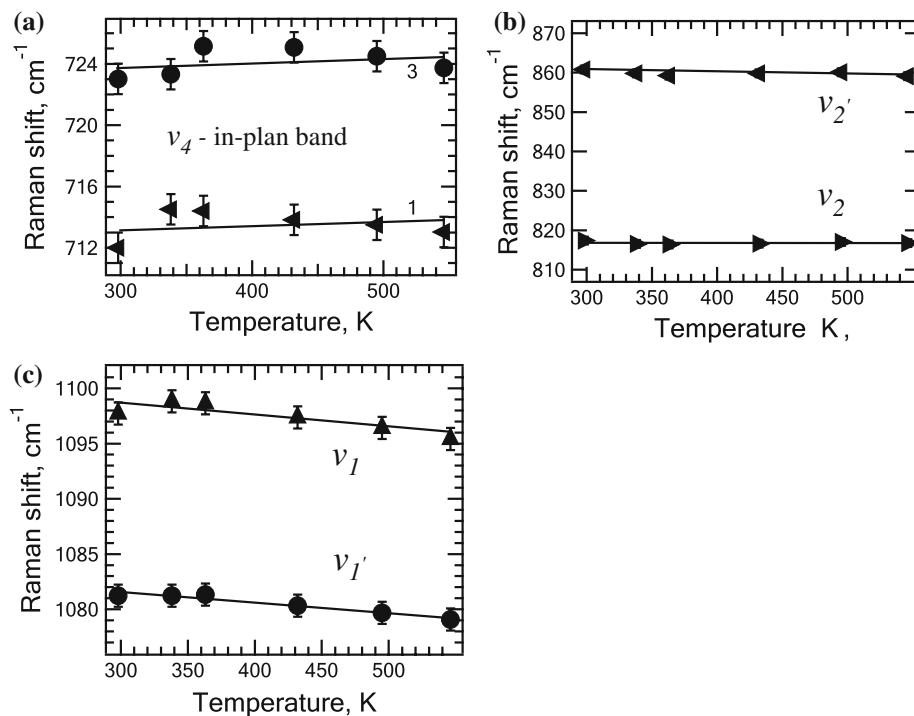


Fig. 8 Raman spectra of internal vibrations at 17.15(20) GPa as a function of temperature: **a** ν_1 and ν_1' -asymmetric stretching vibrations; **b** ν_4 -in-plane band (1 B_{3g} , 2 A_{1g} , 3 B_{2g} , 4 B_{1g}); ν_2 , ν_2' -out-of-plane bands; 7, 8 two additional bands. Spectra are vertically offset for clarity

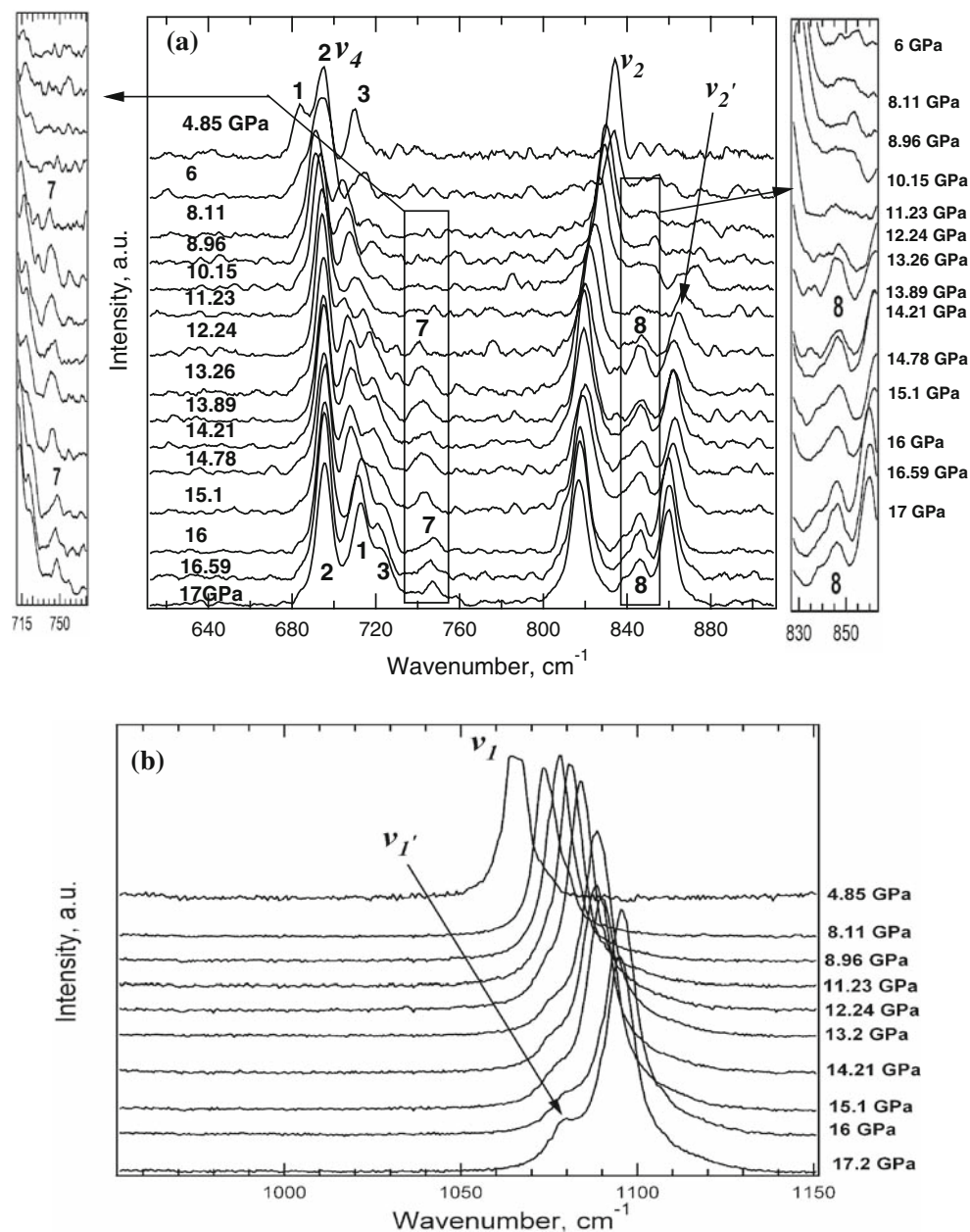
Fig. 9 Temperature dependence of the internal Raman mode frequencies under isobaric conditions at 17.2(2) GPa: **a** ν_4 -in-plane band [1 B_{3g} (filled left triangle), 3 B_{2g} (filled circle); **b** ν_2' -out-of-plane band (filled left triangle), ν_2 -out-of-plane band (filled right triangle); **c** ν_1 -symmetric stretching vibration (filled triangle), ν_1' -symmetric stretching vibration (filled circle). The size of the symbols corresponds to errors in Raman shift and T in **b**



PbCO_3 -II: 2' and 5' (ν_1' and 7 in this work) at 17 and 21 GPa, respectively. In our case the appearance of ν_1' and 7 bands takes place at significantly lower pressure, viz. at about 10 and 17 GPa, respectively. The behavior of bands 6 of Lin and Liu (1997b) and 3 in our work is similar in the pressure range up to 17 GPa, viz. the Raman frequencies increase monotonously with pressure. The onset of band 3 (ν_2' in our work) is at about 9 GPa in both investigations. The behavior of band 4 in the previous work and of our ν_2 is again very similar and the mode softening is observed in the entire pressure range. The total number of measurements in the pressure range 8–12 GPa is only 3 with 2 GPa steps in the work of Lin and Liu (1997b), to be compared with the 10 measurements in our case. The differences with our work might be due to different experimental conditions, e.g. different pressure transmitting media and of a synthetic sample in our case, but natural samples in Lin and Liu (1997b).

The values of dv/dP of the internal modes for PbCO_3 -II are higher than those of the corresponding modes of PbCO_3 -I, thus indicating that the high-pressure polymorph PbCO_3 -II should be more compressible than cerussite (PbCO_3 -I). No doubt this observation is at odds with expectation, however, it is not at all forbidden. A similar behavior is known to occur in BaCO_3 (BaCO_3 -III), and also in the couple of calcite and aragonite (CaCO_3). In the case of BaCO_3 it was rationalized by short Ba–O distances in the a – b plane and long distances perpendicular to that plane (Holl et al. 2000). By comparison the aggregate bulk modulus of aragonite is slightly smaller than that of calcite

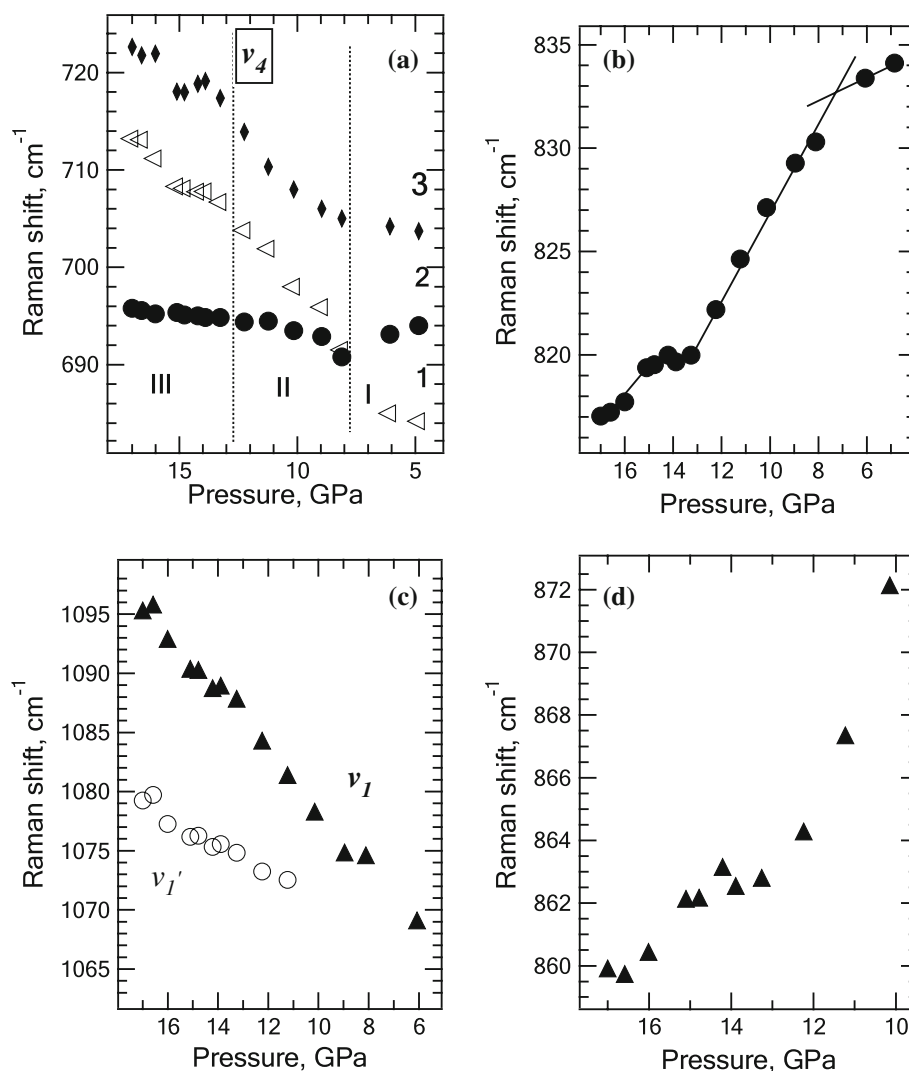
Fig. 10 Raman spectra of internal vibrations as function of pressure at 544(3) K: **a** ν_4 -in-plane band ($1 B_{3g}$, $2 A_{1g}$, $3 B_{2g}$, $4 B_{1g}$); ν_2 ; ν_2' -out-of-plane bands; 7, 8-two additional bands; **b** ν_1 and ν_1' -symmetric stretching vibrations. The spectra were collected during decompression. Spectra are vertically offset for clarity



according to Liu et al. (2005). However, the aragonite used by these authors contained some significant amount of Sr²⁺ (2.5%), with ionic radius larger than that of Ca²⁺ and can deteriorate the elastic moduli of aragonite. At the first transition (6–8 GPa) the general appearance of the spectrum of the internal modes does not change significantly, suggesting that PbCO₃-I and PbCO₃-II could be pseudo-symmetrically related, i.e. that their space groups are probably in group-subgroup relationship. The decreasing splitting of the ν_4 (B_{3g} and A_{1g}) bands indicates changes in the total geometry of the CO₃²⁻ groups, bringing them closer to trigonal symmetry. Phase-III starts to form at about 10 GPa and has smaller dv/dP than phase-II, i.e. lower compressibility. As a result of our investigations a

tentative model of the phase diagram can be constructed (Fig. 12). It contains three phases. Phase-I is cerussite with its aragonite-type structure, stable up to 8 GPa at ambient temperature. The presence of a new high-pressure phase PbCO₃-II could be confirmed. This phase forms reversibly and exists as a pure polymorph only in a small pressure range, from 8 to about 10 GPa at room temperature. The phase-I → phase-II transition is accompanied by the disappearance of the B_{1g} (ν_4) mode and a mode softening of the ν_2 out-of-plane bending, which can be explained by increasing strength of the Pb–O bond with pressure. The negative shift in pressure of the ν_2 band is typical for aragonite-type carbonates (Kraft et al. 1991). The higher frequency shifts of the phase-II modes indicate that the

Fig. 11 Pressure dependence of internal Raman frequencies of PbCO_3 at 544(3) K upon decompression: **a** ν_4 -in-plane band [$1 B_{3g}$ (open left triangle), $2 A_{1g}$ (filled circle), $3 B_{2g}$ (small rhombus), I, II, III the fields of existence of phases I, II, III, respectively; **b** ν_2 -out-of-plane band (filled circle); **c** ν_1 (filled triangle), ν_1' (open circle) symmetric stretching vibrations; **d** ν_2' -out-of-plane band (filled triangle). The size of the symbols corresponds to errors in wavenumber and P



high-pressure polymorph could be more compressible than cerussite as discussed before. The structure of this new phase has not been determined yet.

The formation of PbCO_3 -III has been previously observed by Lin and Liu (1997a, 1997b), and also by Catalli et al. (2005). It sets in at about 10 GPa and is completed at about 16 GPa. Different pressure transmitting media used by Lin and Liu (1997a) (water) and Catalli et al. (2005) could account for the reported differences between both studies. At room temperature a mixture of phases II and III exists in the pressure range from 10 to 16 GPa. There is only one data point available above 700 K and 7.6 GPa, we cannot exclude that this is an outlier and it should be regarded with due caution. The approximate position of the anticipated triple point in the phase diagram was determined as follows: (1) the I–II phase boundary was linearly extrapolated; (2) the end of the II–III phase boundary (at 12.2(2) GPa/544 K) was

connected with the last measured point at 7.6(2) GPa/718 K and extrapolated to determine the crossing point with the I–II phase boundary. The crossing point was then connected with the point at 4 GPa and 1,273 K, which corresponds to phase III of Lin and Liu (1997a). The high-pressure phase PbCO_3 -II in Lin and Liu (1997a) (phase III in this paper) was obtained by quenching from 1,273 K and 4 GPa. This means that PbCO_3 -II in Lin and Liu (1997a) may not be identical with the high-pressure phase observed in situ (22 GPa/298 K) in Lin and Liu (1997b), provided the phase at 4 GPa and 1,273 K is not quenchable. That was the reason to draw a part of the II–III phase boundary as dashed line. It should be noted that PbCO_3 -I possibly does not crystallize in the ‘true’ aragonite-type structure (Durman et al. 1985), possibly due to the presence of the $6s^2$ -lone pair of Pb^{2+} . Hence, the occurrence of PbCO_3 -II could be anomalous with respect to the closed-shell aragonite type carbonates. The question whether a

Table 3 Comparison of dv/dP values of internal vibrations under isothermal decompression at 544 K

Mode	Pressure range (GPa)	dv/dP ($\text{cm}^{-1}/\text{GPa}$)	Mode	Pressure range (GPa)	dv/dP ($\text{cm}^{-1}/\text{GPa}$)
ν_2	17.0–15.2	1.24 (22)	2 ($\nu_4\text{-A}_{1g}$)	17.0–16.0	−0.58 (2)
	15.2–13.2	0.31 (2)		16.0–13.2	−0.18 (5)
	13.2–8.1	2.05 (9)		13.2–9.0	−0.45 (8)
	6.0–4.0	0.59 (8)		8.2–4.0	0.99 (10)
ν_1	17.0–4.0	−2.47 (5)	3 ($\nu_4\text{-B}_{2g}$)	17.0–14.0	−2.28 (40)
ν_1'	17.0–4.0	−1.1 (7)		13.0–8.2	−2.70 (12)
ν_2'	17.0–15.2	1.26 (26)		8.2–4.0	−0.39 (4)
	15.0–13.2	0.38 (3)			
	13.0–10.0	3.76 (40)			
1 ($\nu_4\text{-B}_{3g}$)	17.0–15.1	−3.20 (5)			
	15.1–13.2	−0.79 (18)			
	13.2–6.0	−2.99 (14)			
	6.0–5.0	−0.65 (11)			

Standard deviations of the linear fits to the dv/dP values are given in parentheses

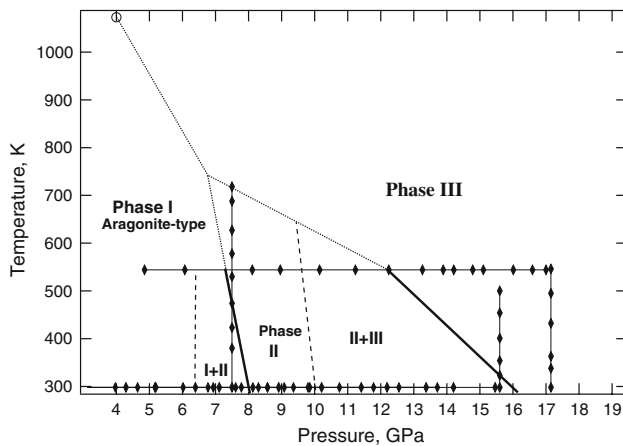


Fig. 12 A model of the tentative phase diagram of the lead carbonate. *I* orthorhombic phase at ambient conditions; *II* new high-pressure phase; *III* high-pressure phase (P2₁22 or P3₁c). *Open circle* denotes data obtained by Lin and Liu (1997a). *Closed connected rhombus* denote points in those were taken data and runs of experiments in this work. The *bold solid lines* are the supposed phase boundaries. The *dotted lines* indicate extrapolation of the phase boundaries. The *dashed lines* indicate the hetero-phase regions I + II and II + III

general phase diagram for aragonite-type carbonates can be constructed remains therefor unanswered.

Conclusions

Our high P – T Raman spectroscopic study of lead carbonate has revealed for the first time a phase transition from aragonite-type PbCO_3 (cerussite) to $\text{PbCO}_3\text{-II}$ occurring at 8 GPa and room temperature. The transition is reversible,

all bands return to their starting position after pressure release. A tentative phase diagram of lead carbonate is proposed. A high P – T X-ray study is proposed to further explore the structure of the new high-pressure polymorph and to refine the position of the triple point in the phase diagram.

Acknowledgments This research was supported by the Deutsche Forschungsgemeinschaft under project number KN 507/5-1 in the framework of the priority program: “Synthesis, ‘in situ’ characterization and quantum mechanical modeling of Earth Materials, oxides, carbides and nitrides at extremely high pressures and temperatures”.

References

- Bachu S (2008) CO_2 storage in geological media: role, means, status and barriers to deployment. *Prog Energy Combust Sci* 34:254–273
- Brenker FE, Vollmer C, Vincze L, Vekemans B, Szymanski A, Janssens K, Szaloki I, Nasdala L, Joswig W, Kaminsky F (2007) Carbonates from the lower part of transition zone or even the lower mantle. *Earth Planet Sci Lett* 260:1–9
- Brown GM (1975) *Composition and petrology of the Earth’s mantle*. McGraw-Hill, New York
- Catali K, Santillan J, Williams Q (2005) A high pressure infrared spectroscopic study of PbCO_3 -cerussite: constraints on the structure of the post-aragonite phase. *Phys Chem Miner* 32:412–417
- Durman R, Jayasooriya UA, Kette SF (1985) Is cerussite an aragonite? Longitudinal optical-transverse optical splitting in the single-crystal Raman spectra. *J Chem Soc Chem Commun* 916–917
- Frech R, Wang EC (1980) The i.r. and Raman spectra of CaCO_3 (aragonite). *Spectrochim Acta* 36A:915–919
- Gibbins J, Chalmers H (2008) Carbon capture and storage. *Energy Policy* 36:4317–4322
- Green HW (1972) A CO_2 -charged asthenosphere. *Nature* 238:2–5

- Holl C, Smyth J, Laustsen H, Jacobsen S, Downs R (2000) Compression of witherite to 8 GPa and the crystal structure of BaCO_3 -II. *Phys Chem Miner* 27:467–473
- IPCC (2005) Special report on carbon dioxide capture and storage. Tech rep, Cambridge University Press, Cambridge, New York
- Isshiki M, Irifune T, Hirose K, Ono S, Ohishi Y, Watanuki T, Nishibori E, Takata M, Sakata M (2004) Stability of magnesite and its high-pressure form in the lowermost mantle. *Nature* 427:60–63
- Janzen H (2004) Carbon cycling in earth systems—a soil science perspective. *Agric Ecosyst Environ* 104:399–417
- Javoy M, Pineau F, Allgre CJ (1982) Carbon geodynamic cycle. *Nature* 300:171–173
- Kepler H, Wiedenbeck M, Shcheka SS (2003) Carbon solubility in olivine and the mode of carbon storage in the Earth's mantle. *Nature* 424:414–416
- Kraft S, Knittle E, Williams Q (1991) Carbonate stability in Earth's mantle: a vibrational spectroscopic study of aragonite and dolomite at high pressure and temperatures. *J Geophys Res* 96:17997–18009
- Lin C, Liu L (1997a) High pressure phase transformations in aragonite-type carbonates. *Phys Chem Miner* 24:977–987
- Lin CC, Liu LG (1997b) Post-aragonite phase transitions in strontianite and cerussite—a high pressure Raman spectroscopic study. *J Phys Chem Sol* 58:977–987
- Liu LG, Chen C, Lin CC, Yang Y (2005) Elasticity of single-crystal aragonite by Brillouin spectroscopy. *Phys Chem Miner* 32:97–102
- Oganov A, Glass C, Ono S (2006) High-pressure phases of CaCO_3 : crystal structure prediction and experiment. *Earth Planet Sci Lett* 241:95–103
- Ono S (2007) New high-pressure phases in BaCO_3 . *Phys Chem Miner* 34:215–221
- Ono S, Kikegawa T, Ohishi Y, Tsuchiya J (2005a) Post-aragonite phase transformation in CaCO_3 at 40 GPa. *Am Mineral* 90:667–671
- Ono S, Shirasaka M, Kikegawa Y (2005b) A new high-pressure phase of strontium carbonate. *Phys Chem Miner* 32:8–12
- Ono S, Kikegawa T, Ohishi Y (2007) High-pressure transition of CaCO_3 . *Am Mineral* 92:1246–1249
- Piermarini G, Block S, Barnett JD, Forman RA (1975) Calibration of the pressure dependence of the R_1 ruby fluorescence line to 195 kbar. *J Appl Phys* 46:2774–2780
- Siidra OI, Krivovichev SV, Filatov SK (2008) Minerals and synthetic Pb(II) compounds with oxocentered tetrahedra: review and classification. *Z Kristallogr* 223:114–125